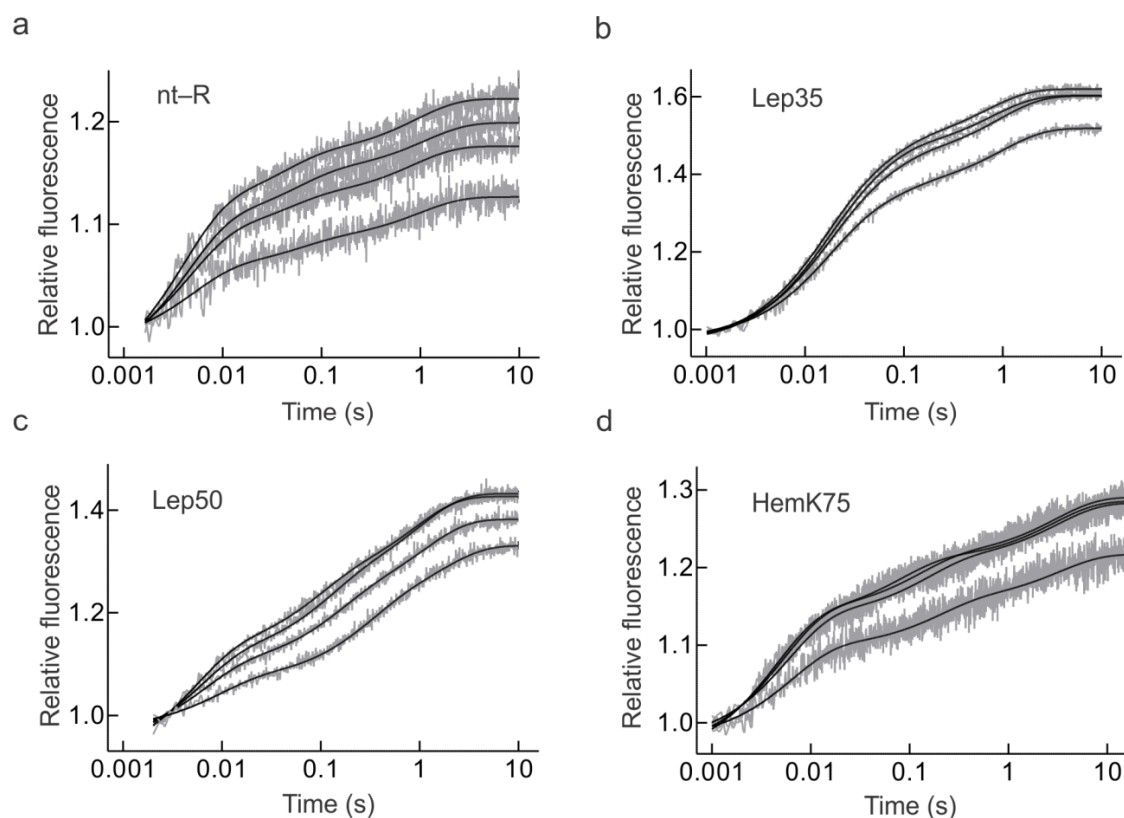
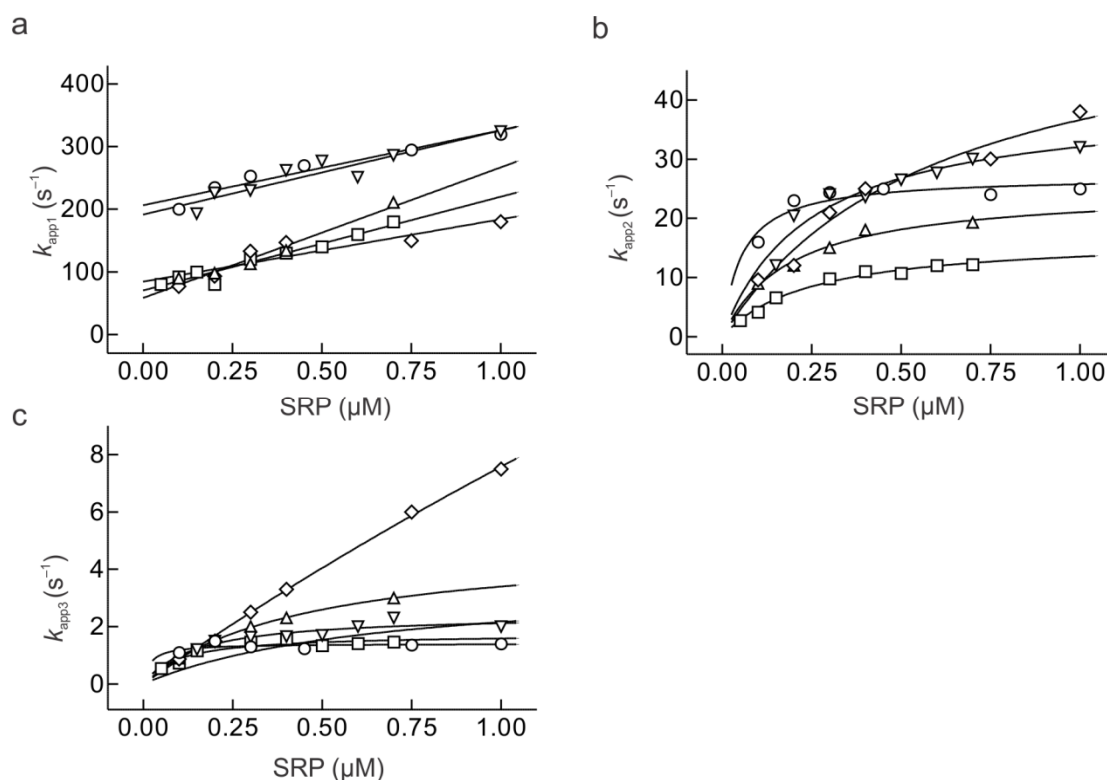


SUPPLEMENTARY MATERIAL

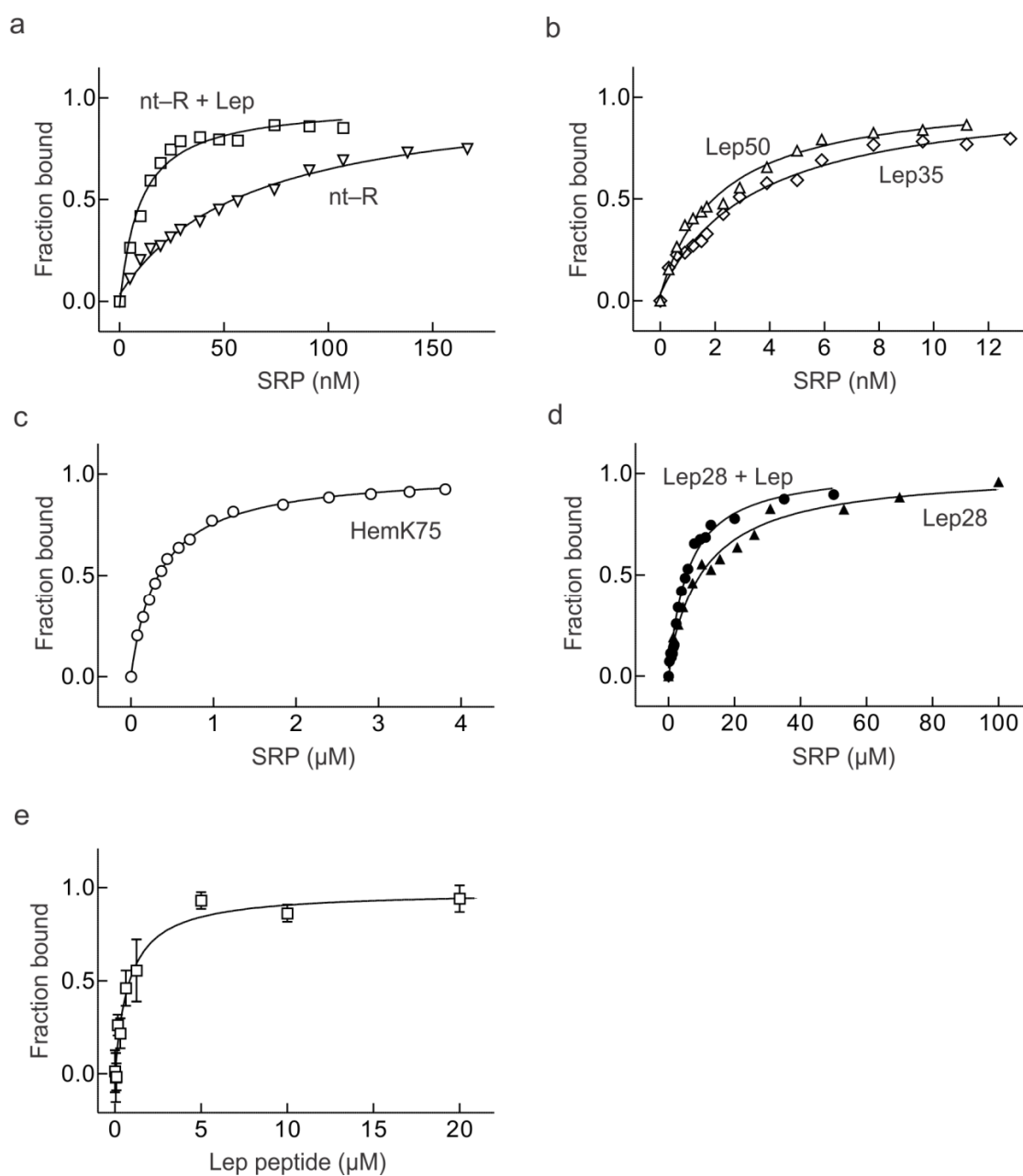
Supplementary Figures



Supplementary Figure 1 Kinetics of SRP binding to ribosomes in different functional states. **(a)** Non-translating ribosomes. MDCC-labeled ribosomes (25 nM) were rapidly mixed with Bpy-labeled SRP present at increasing concentrations (0.1, 0.2, 0.3, 0.75 μM , bottom to top; time courses obtained at 0.45, 0.6, and 1 μM are not shown for clarity). Complex formation was monitored by the increase of Bpy fluorescence due to FRET. **(b)** Lep35-RNC. Stopped-flow experiments were performed as in **(a)**, using MDCC-labeled Lep35-RNCs (25 nM). SRP(Bpy) concentrations: 0.2, 0.3, 0.4, 0.75 μM , bottom to top; time courses measured at 0.6 and 1 μM are not shown. **(c)** Lep50-RNC. SRP(Bpy) concentrations: 0.1, 0.2, 0.3, 0.75 μM , bottom to top; time courses measured at 0.45 and 0.6 μM are not shown. **(d)** HemK75-RNC. SRP(Bpy) concentrations: 0.1, 0.2, 0.3, 0.75 μM , bottom to top. The fitted curves were obtained by global fitting (see text and Online Methods).

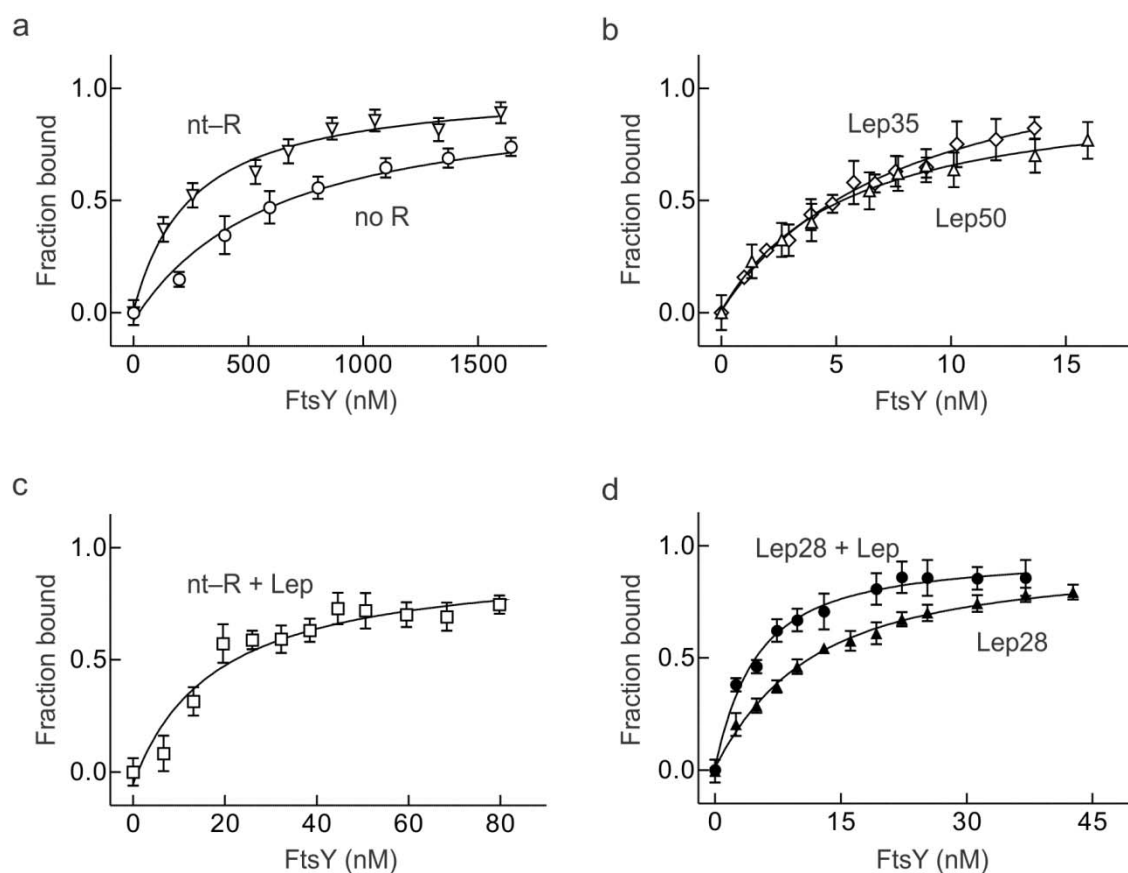


Supplementary Figure 2 Kinetics of SRP binding to ribosomes in different functional states. Concentration dependence of k_{app1} (a), k_{app2} (b), and k_{app3} (c). Time courses of complex formation (**Supplementary Figure 1**) were evaluated by three-exponential fitting (Online Methods). Values of for k_{app1} , k_{app2} , and k_{app3} are plotted against the concentration of SRP. Note that the plots do not allow to directly derive the elemental rate constants of the three-step model obtained by global fitting. Symbols used: Non-translating ribosomes (∇); non-translating ribosomes plus Lep peptide (\square); Lep35-RNC (\diamond); Lep50-RNC (\triangle); HemK75-RNC (\circ).

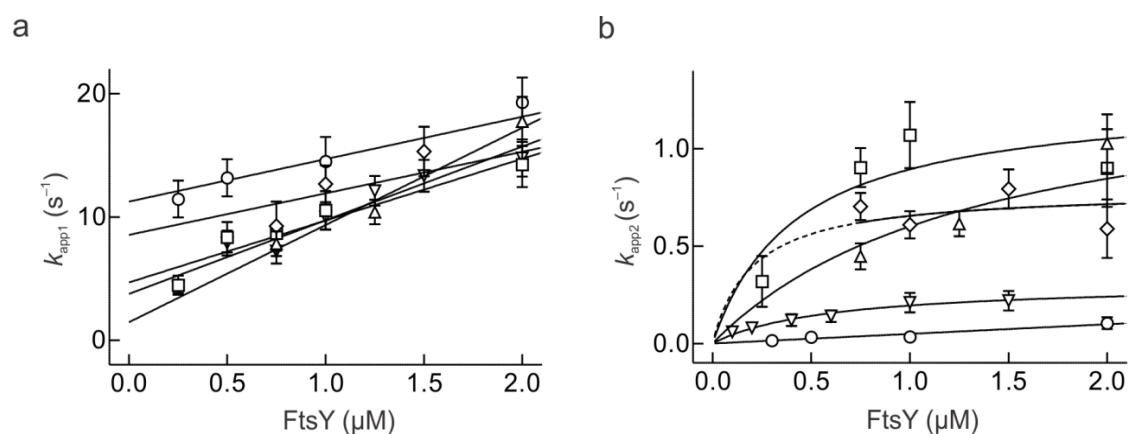


Supplementary Figure 3 Equilibrium titrations. (a) SRP binding to non-translating ribosomes ($K_d = 60 \pm 5$ nM) and to non-translating ribosomes in the presence of Lep peptide (5 μM) ($K_d = 10 \pm 2$ nM). (b) SRP binding to Lep35-RNC ($K_d = 3.5 \pm 0.5$ nM) and Lep50-RNC ($K_d = 2 \pm 1$ nM). (c) SRP binding to HemK75-RNC ($K_d = 350 \pm 30$ nM). (d) SRP binding to Lep28-RNC ($K_d = 11 \pm 2$ nM) and Lep28-RNC in the presence of Lep peptide ($K_d = 5 \pm 1$ nM). (e) Binding of Lep peptide to SRP ($K_d = 0.8 \pm 0.2$ μM). The binding of SRP to ribosomes or RNCs was followed by FRET between labeled ribosomes or RNCs (2.5 nM)

upon addition of increasing amounts of labeled SRP in a FluoroLog 3 spectrofluorimeter (Horiba Jobin Yvon). The binding of Lep peptide to SRP(Bpy) (0.1 μ M) was measured by thermophoresis¹ in buffer A (25°C), using Bpy fluorescence as observable. Binding curves were evaluated by non-linear fitting, taking into account the concentration change of the added ligand due to complex formation by using a quadratic equation for ligand binding to one site.



Supplementary Figure 4 Equilibrium titrations of FtsY binding to SRP and SRP-ribosome complexes. (a) FtsY binding to SRP (50 nM) without ribosomes (no R; $K_d = 0.7 \pm 0.1 \mu\text{M}$) and to SRP bound to non-translating ribosomes (0.5 μM) (nt-R; $K_d = 0.25 \pm 0.05 \mu\text{M}$). (b) FtsY binding to SRP (0.5 nM) bound to Lep35-RNCs (0.5 nM) ($K_d = 7 \pm 2 \text{ nM}$) and Lep50-RNCs (0.5 nM) ($K_d = 5 \pm 1 \text{ nM}$). (c) FtsY binding to SRP (5 nM) bound to non-translating ribosomes (0.1 μM) in the presence of Lep peptide (5 μM) ($K_d = 20 \pm 5 \text{ nM}$). (d) FtsY binding to SRP (10 nM) bound to Lep28-RNC (5 nM) ($K_d = 8 \pm 1 \text{ nM}$) and Lep28-RNC (5 nM) in the presence of Lep peptide (5 μM) ($K_d = 4 \pm 1 \text{ nM}$). Complex formation was followed by FRET, monitoring the fluorescence of SRP(A1x) upon addition of FtsY(QSY). Titrations were performed and binding curves evaluated as in **Supplementary Figure 3**.



Supplementary Figure 5 Kinetics of FtsY binding to SRP or SRP bound to ribosomes in various functional states. Concentration dependence of k_{app1} (a) and k_{app2} (b). Time courses of complex formation were measured by stopped-flow, monitoring FRET between labels on SRP and FtsY and evaluated by three-exponential fitting. Values of k_{app} are plotted against the concentration of FtsY; the third component is very slow and not plotted here (**Supplementary Note**). Elemental rate constants (**Table 2**) were determined by global fitting of time courses. Symbols used: SRP alone (○); SRP bound to non-translating ribosomes (▽); SRP bound to non-translating ribosomes plus Lep peptide (□); SRP bound to Lep35-RNC (◇); SRP bound to Lep50-RNC (△).

Supplementary Note

Analysis of kinetic data

To obtain elemental rate constants, stopped-flow traces (consisting of up to 4000 data points) were first evaluated by one-, two- or three-exponential fitting, as appropriate, using the TableCurve software (Jandel Scientific, San Rafael, USA), yielding up to three k_{app} values, e.g. $k_{\text{app}1}$, $k_{\text{app}2}$, and $k_{\text{app}3}$. Initial estimates for the values of the elemental rate constants, k_1 , k_{-1} , k_2 , k_{-2} , k_3 , and k_{-3} , were obtained from the concentration dependencies of the apparent rate constants (**Supplementary Figs. 2 and 5**) according to described workflows². These values were used as initial guesses for global fitting of the combined datasets of association and dissociation for a given ligand combination. The data were fitted by numerical integration (Matlab; Mathworks Inc., Ismaning, Germany), using one set of differential equations for the time courses of binding and dissociation for each complex. For SRP-ribosome complex formation, the kinetic scheme of **Figure 1c** was used, with variables for the rate constants k_1 , k_{-1} , k_2 , k_{-2} , k_3 , and k_{-3} , and fluorescence factors F_a (fluorescence of free ribosomes), F_c (fluorescence of state 1, **Fig. 1c**), F_d (state 2), and F_e (state 3). The respective K_d values of the complexes, as determined by equilibrium titrations (**Supplementary Fig. 3**), were included in the global fits as fixed values. For the chase data sets, initial concentrations of intermediates were calculated using the initial guesses of the elemental rate constants and varied in each iteration cycle together with the fitted values. R^2 values of the global fits were between 0.995 and 0.999.

The stopped-flow time courses of FtsY binding to free SRP and SRP bound to various ribosome complexes were evaluated in the same way, with the fluorescence parameters for the free ligand, the complex Rib-SRP-FtsY, and the complex Rib-SRP-FtsY*, and an additional rearrangement which was observed upon prolonged incubations. The latter rearrangement was very slow (minutes); it probably represents idling of the complexes due to

the lack of the following targeting steps and was therefore not considered as an on-pathway intermediate. The slow step had no influence on K_d values calculated from rate constants, as forward and backward rate constants were equal. In all cases, global fitting yielded unique solutions for the rate constants as well as for the fluorescence factors.

The distribution of SRP bound to the ribosome between states 1, 2 and 3 was calculated using simulation software based of the values of rate constants k_2 , k_{-2} , k_3 , and k_{-3} ; because only internal equilibria are taken into account, the distribution is independent on the concentrations of free SRP and ribosomes. Effective average dissociation rate constants for the different complexes studied were calculated as average of the respective dissociation rate constants, k_{-1} , k_{-2} , k_{-3} , weighted by the relative population of the three states of these complexes.

Supplementary References

1. Wienken, C.J., Baaske, P., Rothbauer, U., Braun, D. & Duhr, S. Protein-binding assays in biological liquids using microscale thermophoresis. *Nat Commun* **1**, 100 (2010).
2. Bernasconi, C.F. *Relaxation Kinetics*, (Academic press, New York San Francisco London, 1976).